Optimal waste heat recovery in micro gas turbine cycles through liquid water injection

Ward De Paepe[a,*], Francesco Contino[a], Frank Delattin[a], Svend Bram[b,a], Jacques De Ruyck[a]

[a] *Vrije Universiteit Brussel, Dept. of Mechanical Engineering (MECH), Pleinlaan 2, 1050 Brussel, Belgium*
[b] *Vrije Universiteit Brussel, Dept. of Industrial Engineering Sciences (INDI), Nijverheidskaai 170, 1070 Brussel, Belgium*

Abstract

Water injection in the compressor exhaust, to recuperate waste heat, is considered a possible route to improve the electric efficiency and overall performance of the micro Gas Turbine (mGT). Many research exists on water injection in mGTs, however a generic study to determine the optimal route for waste heat recovery is still missing. To determine the optimal cycle settings for waste heat recovery through water injection, we have performed simulations using a two-step method. In a first step, the thermodynamic limit for water injection is sought using a black box method. In a second step, the cycle layout is designed by means of composite curve theory.

This paper summarizes the results of two scenarios. In the first scenario, the black box is considered as adiabatic and no fixed stack temperature is imposed (thus allowing condensation of the exhaust gasses). One of the major concerns when injecting water is the water consumption, which can be compensated in some cases through condensation and recycling the condensate. Therefore, in the second scenario, the cycle is made self-sufficient with water. In this case, the black box is no longer considered adiabatic and heat exchange with the environment is allowed for condensation of the flue gasses.

Black box simulations showed that lowering the stack temperature to

*Corresponding author
Email addresses: wdepaepe@vub.ac.be (Ward De Paepe), fcontino@vub.ac.be (Francesco Contino), fdelatti@vub.ac.be (Frank Delattin), svend.bram@ehb.be (Svend Bram), jdruyck@vub.ac.be (Jacques De Ruyck)

53 °C results in an injection of 17 %wt of water and an increase in electric efficiency of 9 % absolute. To keep the mGT cycle layout simple, low cost and not too complex, a maximum of two heat exchangers was imposed for the heat exchanger network design. Although black box analysis indicated a large potential for water introduction, this potential could not be achieved with the considered networks in this paper. Finally, injection of preheated water was identified as the optimal water injection scheme for waste heat recovery resulting in 4.6 % absolute electric efficiency increase and a final stack temperature of 62 °C. Results of simulations of the second case indicate that the stack temperature needs to be lowered under 26 °C in order to make the cycle self-sufficient with water.

Keywords: micro Gas Turbine, water injection, Black Box method, Composite Curve theory, exergy

---

1. Introduction

Micro gas turbines (mGTs) offer a number of advantages compared to Internal Combustion Engines (ICEs) for small-scale (up to 500 kW_e) power production, for example, a small number of moving parts, compact size and light weight, lower emissions and lower electricity costs [1]. Particularly for the small-scale Combined Heat and Power (CHP) production, mGTs offer great potential [2]. The major drawback is their lower electric efficiency. A lower heat demand mostly leads to a forced shutdown of the mGT, due to the low electric efficiency because producing only electricity with the mGT is more expensive than taking the necessary power from the grid. This forced shutdown reduces the total amount of yearly running hours, making the investment less attractive [3].

A way to improve the overall economic performance of a mGT CHP unit is to improve the electric efficiency of the mGT. Increasing the electric efficiency will make the mGT more competitive against the ICE engine.

Electric efficiency can be improved by increasing the efficiency of the components of the mGT. The two parameters that have potential for efficiency increase are increased Turbine Inlet Temperature (TIT) and higher recuperator effectiveness [4]. Since cooling of the small radial flow turbine is difficult, the TIT can only be increased if thermal resistant – ceramic – materials are introduced in the mGT. The use of these ceramic materials allows for a higher TIT, resulting in considerable energy savings [5]. McDonald

and Rodgers indicated that a ceramic recuperator and ceramic radial turbine are necessary to achieve 40 % efficiency in a 200 kW_e mGT [6]. Campanari and Macchi showed that the high electric efficiency levels achievable with future advanced ceramic mGTs would improve dramatically the economic competitiveness of the application, as well as the primary energy savings and environmental benefits [7]. By using a heat resistant coating technology, Kim and Lee were able to increase the TIT of their home made mGT by 100 °C, resulting in 20 % more power output and 6 % absolute increase in electric efficiency [8]. Increasing the recuperator efficiency is very straight forward, but will however result in a dramatically increase in recuperator size, weight and cost [4]. Pressure drop over the recuperator should be limited, since a 1 % pressure loss increase will decrease the turbine efficiency by 0.33 % absolute [9]. McDonald proposes a basic concept for better heat exchanger design [10]. Finally, Galanti and Massardo indicated that increasing turbine and compressor efficiency by two percentage points would increase the global mGT efficiency without affecting costs in a significant manner [11].

Another way to improve the electric efficiency of the mGT is to introduce water (vapour/liquid) in the cycle. Water injection is considered a successful way to increase electric efficiency of Gas Turbine (GT) cycles [12]. In periods with a low heat demand, the lost thermal power can be recovered by introducing auto-raised steam/heated water inside the mGT cycle, resulting in a more profitable investment [3]. The beneficial effect of steam/water introduction in an mGT on its performance has already been studied several times [13, 14, 15, 16, 17, 18, 19, 20]. Lee et al. showed by means of simulations the beneficial effect of steam injection on the performance of a recuperated mGT cycle [13]. Dodo et al. equipped a 150 kW_e mGT with a Humid Air Turbine (HAT) line and Water Atomizing inlet air Cooling (WAC) line. Experiments showed stable runs at 32 % electric efficiency and reduced NO_x exhaust [14]. Mochizuki et al. performed steam injections experiments on a Capstone C60 mGT. At 60 kW_e and injection up to 6 wt% steam/air ratio, thermal efficiency could be improved by 3 to 4 % [15]. Parente et al. studied the thermodynamic [16] and the thermo-economic performance of the micro Humid Air Turbine (mHAT) [17]. Ferrari et al. injected steam in a hybrid system test rig to study the effect of a steam rich mass flow on engine behaviour. Test results showed that the mGT accepted the injected steam mass flow rate without surge problems [18]. More recently, Wei and Zang experimentally investigated the off-design behaviour of a small-sized (25 kW_e) HAT cycle. Test results at constant fuel flow rate and constant

TIT indicated significant power output increases of 3 kW_e and 9.5 kW_e [19]. Our research group simulated [3] and validated the effects of steam injection on the performance of a Turbec T100 mGT [20]. Recently, the authors of this paper indicated that by converting the T100 mGT into a mHAT, electric efficiency will increase by 2 % absolute [21].

None of the previous mentioned studies however identified the most optimal route for water introduction in a mGT cycle to recuperate the lost thermal power. Our research group developed a general two-step approach for optimal humidified GT cycle development [22]. In this procedure, the thermodynamic potential of water injection is first determined using an adiabatic black box method. In a second step, the final cycle layout is designed, using composite curve theory. This two-step approach showed its potential by identifying the HAT, as proposed by Rao [23], as the most optimal layout for a humidified cycle. This two-step approach also led to the development of a new humidified GT, without using a saturation tower, the REgenerative EVAPoration cycle (REVAP®) [24]. This cycle has about the same net efficiency as the HAT cycle (54 %) [12]. We applied this two-step method to the mGT cycle to identify the most optimal way for water introduction in a mGT cycle.

In this paper, the results of two different scenarios concerning the water injection in a mGT, using the two-step procedure, are presented. In the first scenario [Scenario 1 (S1)], the black box is considered as adiabatic and no fixed stack temperature is imposed (thus allowing condensation of the exhaust gasses). Since water consumption is a major issue for mixed air/water GTs, in the second scenario [Scenario 2 (S2)], the cycle is made self-sufficient with water. In the first scenario (S1), we did not control the amount of condensed water. In the second scenario (S2), we add a new constraint to condense exactly the amount of water introduced in the mGT cycle (not all water present in the flue gasses). The main goal of S1 and S2 is to identify the thermodynamic limit for water introduction in a mGT under these considered boundary conditions. By using composite curve theory, different ways for water introduction in a mGT cycle for waste heat recovery could be developed. The performance of each cycle is then compared with the black box results in order to check if the full potential for waste heat recovery is exploited. The cycle that approaches the black box results the closest is then identified as the most optimal way for waste heat recovery through water injection in a mGT. Both selection procedure and final cycle lay-out will be presented in this paper.

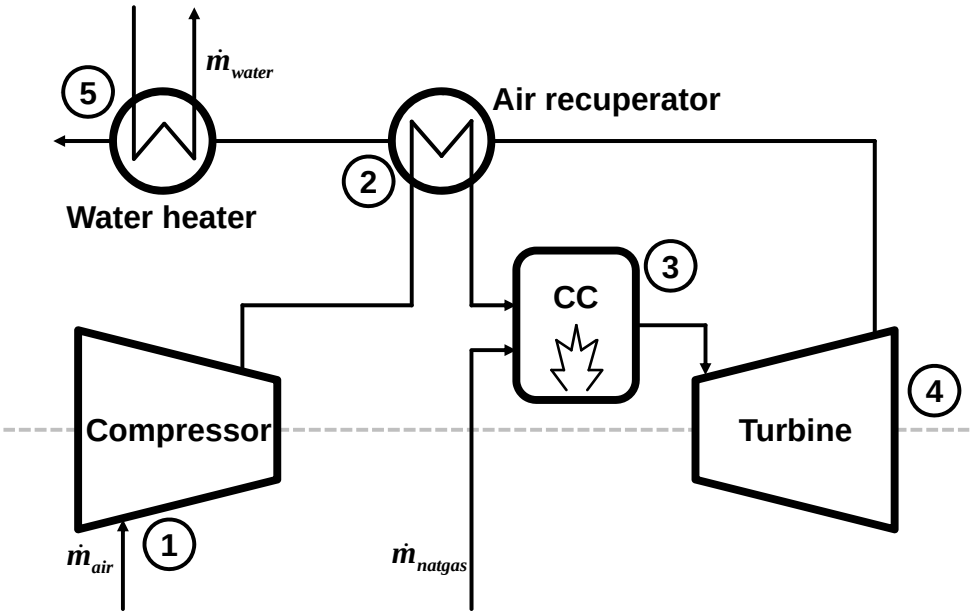

Figure 1: The compressed air (1) is preheated by the flue gasses in the recuperator (2) and heated in the combustion chamber (3) by burning natural gas. Expanding the hot gasses over the turbine provides the power (4). Finally, the residual hot flue gasses are used to heat water for domestic heating purposes (5).

2. Approach

The Turbec T100 microturbine CHP system is a typical recuperated mGT system (Figure 1). The inlet air enters the compressor (1), where it is compressed. The compressed air is preheated in the air recuperator by the hot flue gasses (2). In order to obtain the best performance, the compressed air is heated until maximal TIT (950°C) by burning natural gas in the combustion chamber (3). The hot gasses will expand over the turbine (4), which is connected to the compressor and a high-speed generator. After preheating the compressed air, the excess heat, available in the flue gasses, is used to heat water for heating purposes (5). A brief summary of the mGT performance is given in Table 1.

By changing the shaft speed, the T100 mGT control system keeps the

Table 1: Nominal specifications of the Turbec T100 mGT [25]

Electric power	100 kW_e
Thermal power	167 kW_{th}
Electric efficiency	30 %
Thermal efficiency	50 %
Shaft speed	70 000 rpm

produced electric power output constant at a user defined set point (between 60 and 100 kW_e). The compressor and turbine operate thus at the same variable shaft speed, which results in variable mass flow rate and pressure ratio. Besides the shaft speed, the fuel flow rate is also controlled in order to maintain TIT at is maximal value. The variable shaft speed and constant TIT allow the T100 to operate at high part load electric efficiency [25]. The produced thermal power can be controlled by routing part of the exhaust gasses directly to the stack and thus bypassing the water heater. This will however lower the thermal efficiency of the mGT, which characterizes the major problem of the mGT as CHP. Due to the lower part load thermal efficiency, mGT operation is mainly heat driven.

The current paper summarizes the results of two series of water injection simulations, performed on the Turbec T100 mGT. The study is intended to be general on waste heat recovery in mGT cycles, similar to the cycle depicted in Figure 1. This includes all recuperated Brayton cycles, using single stage radial compressor with no intercooling, operating at variable shaft speed and thus variable pressure ratio. This is the major difference between the study presented in this paper and the study previously presented by our research group, were a constant pressure ratio was used [24]. For the simulations, we preferred to use real data from a Turbec T100 mGT, since it is very important to simulate correct the behaviour of the compressor at variable shaft speed. The Turbec T100 mGT was selected since it is representative for recuperated mGT cycles operating at variable shaft speed and the off-design behaviour is well-known due to previous experiments [26].

The adopted analysis method was an earlier developed two-step procedure for the design of mixed air/water power cycles [22]. In this procedure, the thermodynamic potential of water injection is first studied, using the black box method. As mentioned in the introduction, in the first scenario (S1), the black box is considered adiabatic and no fixed stack temperature is

imposed (thus allowing condensation of the exhaust gasses), while in the second scenario (S2), the cycle is made self-sufficient with water. So the major difference between S1 and S2 is that in S1, we did not control the amount of condensed water, while in S2, we add a new constraint to condense exactly the amount of water introduced in the mGT cycle (not all). In S2, the black box is no longer considered adiabatic and heat exchange with the environment is necessary to condense the flue gasses. In the second step, the final cycle layout is designed, using composite curve theory. In this step, the black box is realized by developing a heat exchanger network. Although black box results of S1 and S2 ensure theoretical feasibility due to the overall positive exergy destruction, the final heat exchanger network design corresponding to this potential will probably be too complex and too costly for mGT applications. The eventual thermodynamic feasibility of the heat exchanger network can be verified by inspecting the composite curves. The final result of this second step is the design of the most optimal mGT cycle layout for waste heat recuperation using water injection.

3. Method

All simulations, presented in this paper, are performed using the Aspen® plus simulation engine (version 2006.5) [27]. Simulations were performed at constant nominal power of the T100 mGT (100 kW_e). In the following subsections, first the modelling of the T100 mGT in Aspen® will be discussed. Next to the modelling of the mGT components, the black box simulation method and exergy analysis of scenarios S1 and S2 are discussed. Finally, additional information about the composite curve theory, used to design the heat exchanger network, is given.

3.1. mGT components modelling

For the modelling of the mGT in the Aspen® plus simulation engine, an adapted version of previous developed models of the dry and wet mGT [3] are used. These models were validated in [20].

The existing controller of the T100 mGT is implemented in the Aspen® models. The controller keeps the electric power and TIT constant by adapting the compressor shaft speed and natural gas flow. In the Aspen® models, constant electric power and TIT are set as design specifications. By varying shaft speed and natural gas flow, the Aspen® solver can converge to a solution, respecting the design specifications.

For the modelling of the compressor, a generic compressor map was used. When water is injected in the cycle, the total mass flow rate through the turbine will increase, resulting in a higher turbine/electric power. To keep the produced electric power constant, rotation speed is decreased, resulting in a lower compressor mass flow rate (off-design). Since it is the goal of this paper to find the limit for water injection in the mGT, the operation point of the compressor will move away from its optimal dry operating point, resulting in a lower isentropic compressor efficiency. For this reason, areas of constant compressor efficiency were implemented in the Aspen® compressor map.

In the model, the turbine is choked, which is expressed as follows [28]:

$$\frac{\dot{m}_{\text{turb}}\sqrt{\text{TIT}}}{\text{PIT}} = A\sqrt{\frac{k_{\text{turb}}}{R}\left(\frac{2}{k_{\text{turb}}+1}\right)^{\frac{k_{\text{turb}}+1}{k_{\text{turb}}-1}}}. \tag{1}$$

Due to the injection of water, the heat capacity ratio (k_{turb}) in Equation 1 will change (0.1 % per 0.01 $\text{kg}_{\text{steam}}/\text{kg}_{\text{air}}$), resulting in a different chocking value. Next to the chocking condition, the isentropic efficiency of the turbine will also change due to water injection. Dry turbine efficiency is equal to 0.85 and is compensated using the following formula (for details, see [16]):

$$\frac{\eta_{\text{is}}}{\eta'_{\text{is}}} = \frac{k'-1}{k'-1}\sqrt{\frac{k'+1}{k+1}\frac{1-1/\beta^{\gamma'}}{1-1/\beta^{\gamma}}}. \tag{2}$$

In Equation 2, the apex ($'$) refers to the properties at standard air composition. γ is defined as $(k-1)/k$. Both corrections were added to the simulation model.

The heat exchangers were modelled with generic heat exchanger models. Pressure loss over the cold side of the heat exchange network was set to 3 % of the total pressure, for the hot side, a pressure drop of 40 mbar was imposed. These losses correspond to the actual losses in the dry cycle of the T100 mGT. The pressure loss is considered as a design specification and it is kept constant to allow for a systematic comparison of all simulation results. The imposed 3 % pressure loss is a trade-off between the cost of the heat exchangers (which is related to their size) and the efficiency of the installation (which is related to the imposed pressure drop). Dry simulations in our Aspen® model showed that increasing pressure loss between compressor outlet and turbine

inlet from 3 to 4 % will result in a 0.32 % absolute efficiency loss. This is comparable to the 0.33 % absolute efficiency loss mentioned by Lagerström and Xie [9]. Each final cycle design will thus require the development of specific heat exchangers to meet the design conditions for heat transfer and pressure drop.

3.2. Black box analysis

For the simulations performed in the first step of the two-step method, all heat exchangers in the mGT layout from Figure 1 were removed and replaced by a black box. For the first scenario (S1), an adiabatic black box was used, for the second scenario (S2), heat exchange with the environment (heat sink) was allowed, since the flue gasses needed to be cooled in order to make the cycle self-sufficient with water. In Aspen®, a straightforward implementation of a black box does not exist. Our research group [22] proposed an alternative, by generating a network of generic heaters and coolers, that would act as a black box system. A modified version of the proposed black box network in [22] is used for the simulations performed for this paper. The T100 mGT has only one compressor stage, so there is no intercooling, which reduces the number of heaters and coolers in the network to two.

For S1, the black box network design as depicted in Figure 2 has been used. For the first scenario (S1), the water is first injected in the compressed air. Before entering the combustion chamber, the air/water mixture is pre-heated in the HEATER. The flue gasses coming from the turbine are then cooled in COOLER before they are ejected through the stack. When expressing conservation of the energy over the black box, the correlation between the thermal power of the heater and cooler can be expressed as:

$$\dot{Q}_{\mathrm{COOLER}} + \dot{Q}_{\mathrm{HEATER}} = 0 \tag{3}$$

In the black box, there are three parameters that can be controlled, but only two degrees of freedom, since the compressor outlet mass flow rate, pressure and temperature and the Turbine Outlet Temperature (TOT) are controlled by the mGT control system (power output and TIT control). If the temperature difference between the cold side outlet and hot side inlet of the black box is imposed (hot pinch), together with the stack temperature, and taking into account the energy balance in Equation 3, the amount of water that must be injected is set.

The goal of S2 is to check the possibility to make the cycle self-sufficient for water. The major disadvantage of mixed air/water GTs is the large water

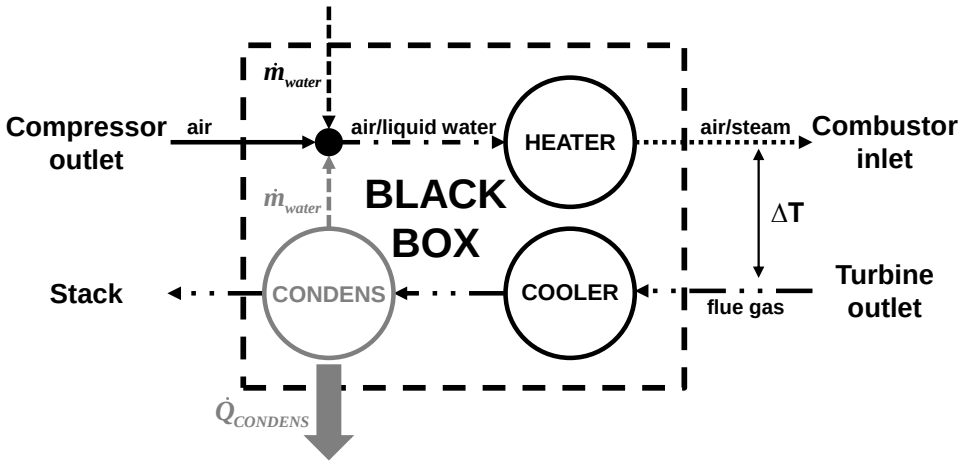

Figure 2: Black box layout used for simulations of Scenario 1 (S1) and Scenario 2 (S2, grey parts).

consumption [29]. By introducing a condenser in the cycle, it is possible to recover all the injected water [30]. For this case study, the black box layout is thus slightly adjusted (additional grey parts in Figure 2). The flue gasses coming from COOLER in Figure 2 are cooled further in CONDENS to get condensation of the water present in the flue gasses. The excess heat of the CONDENS-cooler ($\dot{Q}_{\mathrm{CONDENS}}$) is rejected to the environment. Again, three parameters can be controlled in the black box, while there are only two degrees of freedom. In this case, if we impose the hot pinch and the heat disposal to the environment, the stack temperature and the amount of circulating water are set, due to the closed loop.

The boundary conditions used for the black box simulations of S1 and S2 are shown in Table 2. The stack temperature during simulations is variable. Rather than applying a specific stack temperature to the black box system, it was decided to control the amount of injected water. Simulations showed that controlling the amount of injected water allows Aspen® to reduce the convergence time, especially when condensation appears in the flue gasses.

Table 2: Boundary conditions used in the black box simulations of Scenario (S1) and Scenario 2 (S2).

Compressor	
Pressure ratio	Variable [1]
Isentropic efficiency	Variable [1]
Inlet air temperature	15 °C
Turbine	
Turbine back pressure	50 mbar
Isentropic efficiency	Variable [2]
Turbine Inlet Temperature (TIT)	950 °C
Combustion chamber	
Combustor pressure loss	5 %
Heat recovery system	
Cold side pressure loss	3 %
Hot side pressure loss	40 mbar
Water injection pressure loss	0.5 %
Hot inlet/cold outlet temperature difference	50 °C
Stack temperature	Variable [3]
Feed water inlet temperature	15 °C
Fuel (methane)	
Fuel temperature	30 °C
Fuel pressure	6 bar
Lower Heating Value	50 MJ/kg
General	
Produced electric power	100 kW_e

[1]Generic compressor maps were used in the simulations.

[2]The isentropic efficiency depends on the water content of the working fluid, but TIT is constant.

[3]The final stack temperature depends on the amount of injected water.

3.3. Exergy analysis of the black box systems

The exergy destruction in the black box as a fraction of the total exergy content of the fuel is defined as follows:

$$BB^{\text{dest}} = \frac{\sum_{\text{in}} \dot{E}x - \sum_{\text{out}} \dot{E}x}{\dot{E}x_{\text{fuel}}}. \tag{4}$$

Exergy efficiency is defined as the ratio between the sum of the exergy of the streams that gain exergy, and the sum of the exergy of the streams that lose exergy:

$$BB^{\text{eff}} = \frac{\sum_{\text{gain}} \Delta \dot{E}x}{\sum_{\text{loss}} \Delta \dot{E}x}. \tag{5}$$

For both S1 and S2, the exergy efficiency is thus reduced to the ratio between the exergy gain of the compressed air and the exergy loss of the flue gasses. Since the water injection system is designed to recover wast heat, the condensation heat, which is exposed to the environment, is seen as a loss and is therefore not introduced in the exergy balance. For the calculation of the exergy of the different streams, an in-house Fortran procedure has been used [22].

For each amount of injected water, exergy destruction and efficiency were calculated. In literature, values of a global exergy destruction of minimal 5 % and a black box exergy efficiency as high as 93 % are used as limits for the heat transfer systems [31]. Crossing these limits will lead to unrealistic designs, too difficult to realize with real heat exchangers.

3.4. Heat exchanger network design

For the final design of the heat exchanger network, based upon results of black box analysis, composite curve theory was used [32]. For the composite curves, a minimum pinch of 10 °C was set as design condition. Altered networks of evaporators and heaters and coolers were proposed until a positive minimum approach temperature of 10 °C was obtained between the composite curves. For all simulations, the same boundary conditions as given in Table 2 and used for the black box simulations were used. For the actual heat exchangers, an additional condition was used: 10 °C minimal temperature difference between the hot exhaust and cold inlet. Furthermore, generic heat exchanger models were used, since the actual design of the heat exchangers is beyond the scope of this paper.

Possible heat exchanger network designs for waste heat recovery in a mGT were taken from large scale humidified GTs. Jonsson and Yan divided these humidified GTs into three categories [12]:

- GTs with injection of water that evaporates completely;

- GTs with injection of steam;
- GTs with injection of water in a humidification tower, with a recirculating water loop.

The first category includes not only systems with water injection behind the compressor with recuperation, but also water injection at the compressor inlet for power augmentation on hot days and water injection in the compressor for intercooling. In this paper, the two latter systems are not taken into account and neither is steam/water injection in the combustion chamber. Water/steam is always introduced behind the compressor and before the combustion chamber (Figure 2). Both inlet and intercooling techniques can be applied on a mGT to increase the power production or efficiency by decreasing the compressor work. These techniques are however not suited for the recovery of available waste heat in the hot exhaust gasses and are therefore not included in this study. Water/steam injection in the combustion chamber will increase the power production and decrease NO_x emission. The waste heat recovery is however limited, since the water is introduced after the regenerator. Finally, to keep the cycle layout simple and easy to operate and reduce the capital cost, it was decided to limit the amount of heat exchangers to maximal two.

4. Results

In this section, first three possible problems related to water injection in a mGT are discussed: surge margin reduction, combustion stability and water condensation from the flue gasses. In the second part, black box simulation results of S1 and S2 are discussed. Finally, the optimal heat exchanger network design is proposed.

4.1. Water injection related issues

The Turbec T100 mGT operates at constant electric power output condition. As mentioned before, the mGT controller will keep the power production constant by decreasing the compressor mass flow rate through a reduction in the shaft speed. Since water will be injected after the compressor, but before the turbine, there is an unbalance in mass flow rate, resulting in a higher turbine power and additional produced electric power. To keep the power output constant, the shaft speed is reduced. This shaft speed reduction causes a lower pressure ratio and air mass flow rate. The shaft

speed reduction will shift the compressor operation point to the surge limit. According to Walsh, a minimal surge margin of 15-20 % is necessary for low-pressure compressors in power generation applications [33].

Due to the injection of water, some problems with combustion stability may arise. The combustion instabilities can lead to reduced combustion efficiency and an increased emission of carbon monoxide and unburned hydrocarbons [12]. The addition of water has, however a positive effect on NO_x exhaust [34]. Belokon et al. showed that combustion efficiency remains high (above 95 %) for a water content up to 18 wt% [35]. According to Hermann et al., the limit for combustion is 33 wt% of water in the gasses; beyond this limit, combustion becomes unstable due to the high CO levels [36].

Experimental results of full water recovery in a steam injection GT [37] and a HAT cycle [38] also showed that the condensed water contained several contaminants (ions) and had a certain level of acidity due to the presence of dissolved CO_2. Water treatment is thus necessary before the water can be recycled. In addition, once the temperature of the flue gasses drops below dew point temperature, an acidic environment is created due to the water condensation. The heat exchangers and stack need to be protected against corrosion. The water condensation will only happen at low temperature, therefore standard treatments or materials used in condensing boilers can be used in this application.

4.2. Black Box

For both S1 and S2, water and compressed air are mixed before entering the HEATER (Figure 2). Depending on the amount of water, the mixture entering the HEATER is either humidified air, fully saturated air or saturated air that still contains liquid water droplets. All remaining droplets however will evaporated in the HEATER. Final combustor inlet temperature varies from 629 °C (0 kg/s water injection) till 675 °C (0.09 kg/s water injection) assuring no water droplets will enter the turbine.

With increasing injected water, the stack temperature in S1 decreases linearly (Figure 3). The more water is injected, the more heat needs to be exchanged between the flue gasses and the wet compressed air in order to reach a combustor inlet temperature such that the hot pinch temperature is 50 °C. The stack temperature reduction continues until 53 °C is reached. At this point, the water inside the flue gasses starts to condensate, resulting in an extra release of heat. The total amount of water condensed is also shown in Figure 3. For this reason, it was decided to use the injected water mass

flow rate as variable in the black box calculations and to calculate the stack temperature, which allowed simulating beyond the point of condensation. If the stack temperature was set to 53 °C, no convergence in Aspen® was reached, since there are multiple solutions.

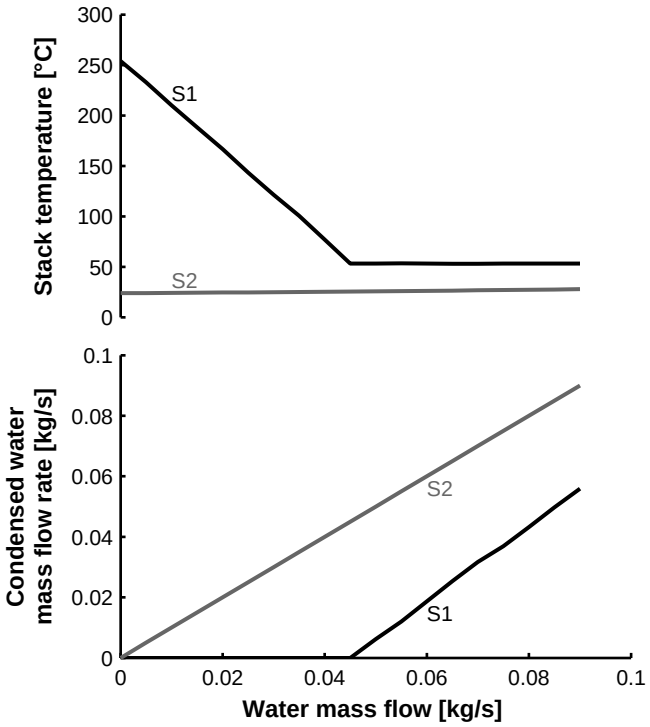

Figure 3: In Scenario 1 (S1), stack temperature reduces linearly with increasing injected water mass flow rate till 53 °C, when water condensation releases extra heat, resulting in a nearly constant stack temperature. Stack temperature slightly increases for Scenario 2 (S2) with increasing water injection.

The stack temperature in S2 slightly increases with increasing water mass flow rate (from 24 °C at 0.005 kg/s to 28 °C at 0.09 kg/s) (Figure 3). The increasing stack temperature is a result of the decreasing air mass flow. The higher the water injection mass flow rate, the more the mGT controller will reduce the rotation speed and thus the air mass flow rate. The lower the air mass flow, the less water can be evaporated in the saturated air, which results in a higher stack temperature when all necessary water is condensed. The temperature rise is however slightly slowed down since less natural gas

is burned. The amount of condensed water in S2 corresponds to the amount of injected water, since it was the goal to make the cycle self-sufficient for water in S2.

Simulations of S1 and S2 were stopped at an injection of 0.09 kg/s of water for both scenarios (Figure 3). At this point, the compressor had reached his surge limit (Figure 4). The impact of the water injection on the compressor performance is shown on Figure 4. As mentioned before, the operating point shifts towards the surge margin. Surge margin is reached when 0.09 kg/s of water is injected in the cycle, corresponding to a water fraction of 17 wt%, which is still below the limit set by Hermann et al. for combustion stability [36]. In order to reach this 0.09 kg/s of water injection, the compressor needs to be redesigned in order to obtain a sufficient surge margin of 15-20 % [33].

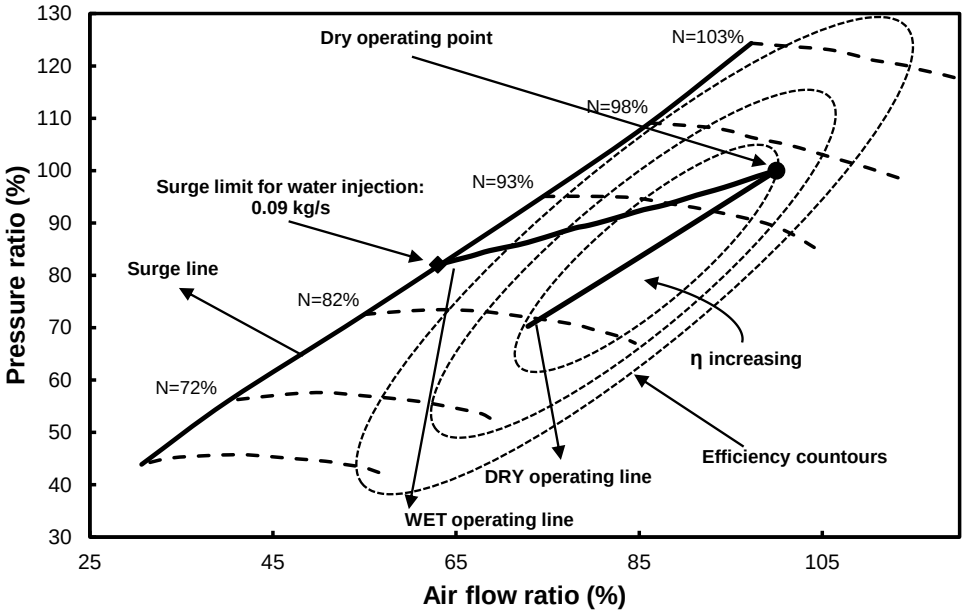

Figure 4: Compressor map showing the shift of the wet operating point towards the surge limit due to water injection.

For all applied water mass flow rates, the exergy destruction and efficiency are below the limits from literature [31] (Figure 5). For increasing injected water mass flow rates, the exergy efficiency of the black box from S1, decreases first, while destruction increases. Afterwards, exergy destruction

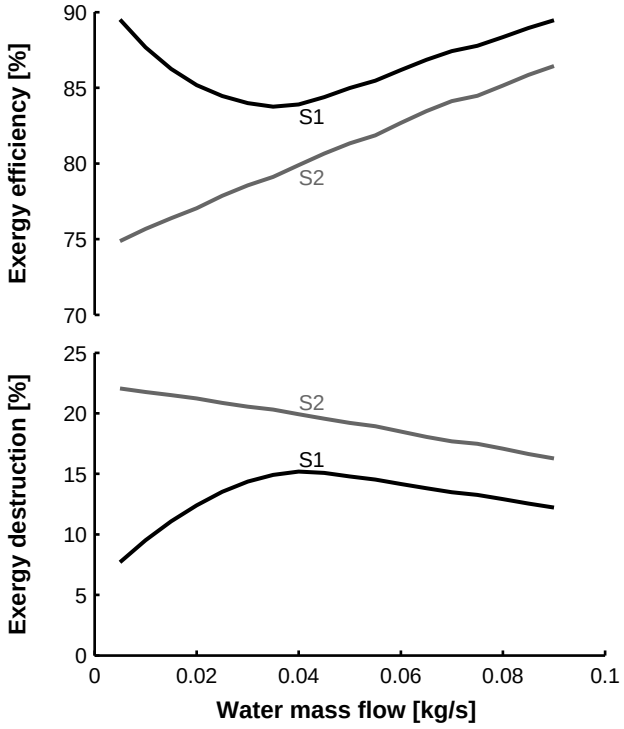

Figure 5: Exergy efficiency and destruction remain below the limit from literature for all different amounts of injected water.

starts to decrease while exergy efficiency increases again. Exergy efficiency of S2 increases with increasing water mass flow, while exergy destruction decreases. The higher the amount of injected water, the more energy is recuperated in the HEATER-COOLER system and less is lost in the cooling process to condensate the flue gasses. This explains the increasing efficiency and decreasing destruction. One can also see that the exergy efficiency of the black box in S2 is lower than the exergy efficiency of the black box in S1, which is due to the lower stack temperatures in S2 (see Figure 3). Flue gasses are cooled to get condensation of the water; however, the exergy of this cooling process is not used, resulting in an extra loss, explaining the lower exergy efficiency.

The behaviour of exergy efficiency and destruction in S1 can be explained by looking to the exergy fluxes entering and leaving the black box, shown in Figure 6. The exergy flow of the feed water from S1 is not shown on Figure 6,

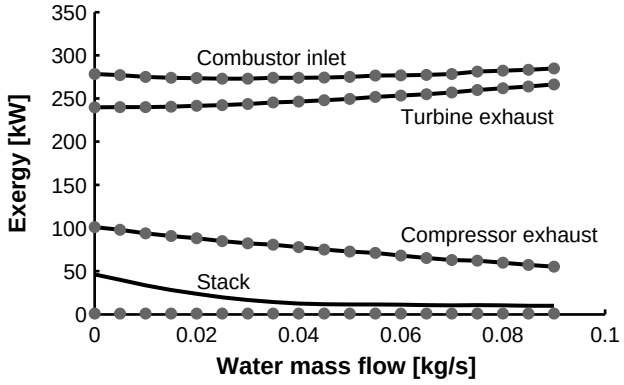

Figure 6: The different exergy flows of the black box system explain the difference in exergy efficiency and destruction between S1 and S2. Results of S1 are shown using lines, while the corresponding results of S2 are shown using symbols.

since the water is introduced in the black box in its dead state (15 °C, 1 bar, liquid phase) and has therefore no exergy.

The different behaviour of the different exergy flows from Figure 6 can be explained as follows:

- With increasing water injection, the exergy flow through the turbine exhaust increases, due to the higher water content of the flow. Because of the higher water content, the TOT is also slightly higher, since TIT is kept constant by the mGT control system. The control system however also reduces the mass flow rate, which limits the exergy flow increase.

- Exergy flow at the combustor inlet however remains more or less constant. The increasing exergy flow because of the higher temperature and water content is compensated by the lower pressure and mass flow rate, resulting from the lower rotation speed set by the mGT controller.

- The lower pressure ratio, mass flow rate and compressor outlet temperature result in a decreasing exergy flow entering the black box from the compressor outlet.

- Since the stack temperature is gradually reduced with increasing water injection, the outgoing exergy flow through the stack is also reduced.

From the injection of 0.045 kg/s of water on, the stack temperature remains nearly constant due to the condensation of water, resulting in a stabilisation of the exergy flow.

Using previous information, exergy efficiency and destruction of S1 of Figure 5 can be explained. The exergy flow of the stack decreases faster than the exergy flow of the compressor outlet. The exergy flow increase of the turbine exhaust is larger than the one at the combustor inlet. This results in decreasing exergy efficiency, while the exergy destruction of the black box increases. When reaching a stack temperature of 53°C, the exergy loss through the stack remains constant, resulting in increasing exergy efficiency and decreasing exergy destruction.

Comparing exergy flow of S1 with S2 shows only one difference. Exergy flows of the combustor inlet, turbine exhaust and compressor outlet remain constant at the same injected water fraction, while the exergy flow of the stack is in S2 much smaller than S1. The stack temperature of S2 is low compared to the stack temperature of S1 (Figure 3). On top of this lower temperature, the amount of water vapour present in the flue gasses is much lower, due to the condensation of the necessary water, resulting in a very low exergy flow.

The electric efficiency of the mGT will increase, as expected, with increasing injected water mass flow rate (Figure 7). Although, exergy efficiency first decreases and then increases; this has no effect on the global efficiency of the mGT. The absolute efficiency rise depends on the amount of injected water. The non-linear efficiency increase is a result of the transformation of the compressor map into working lines. The efficiency slightly decreases between 0.070 and 0.075 kg/s water injection by 0.01 %. Due to the increasing water mass flow rate, the mGT control system will reduce the compressor rotation speed to keep the produced power constant. By doing so, the compressor shifts further away from its design operating point, resulting in a decreasing compressor efficiency. Between 0.070 and 0.075 kg/s, compressor efficiency drops from 77.4 % to 76.0 %. In this case, the positive effect of extra water addition is fully cancelled by the lower compressor efficiency.

At an injection rate of 0.09 kg/s, the absolute efficiency rise amounts 9 %. Comparing results of S1 (line) with S2 (diamonds) shows that there is no difference between the electric efficiency, as could be expected. In the black box system of S2, the feed water flow is replaced by a condenser that will provide the necessary water. The heat output of this condenser is not

used in the system; so finally, there is no difference between S1 and S2 for the mGT performance. In the actual power plant, when the losses of the auxiliaries needs to be taken into account, there will be a difference, since energy is needed for the water treatments or for the cooling of the flue gasses to get condensation (and possible also water treatment).

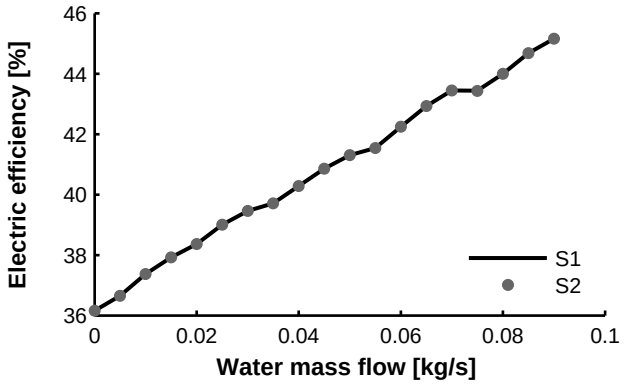

Figure 7: Electric efficiency increases with increasing injected water mass flow rate for S1 (line) and showing good accordance with efficiency increase from S2 (circles).

From the results of the electric and exergy efficiency, one can conclude that condensing the exhaust gasses needs to be accomplished with an external heat sink. None of the transferred exergy can be used in the system. The final design of the heat exchanger network is the same as for S1, with an additional cooler on the flue gas flow to cool the flue gasses to get condensation of the required water.

4.3. Heat exchanger network design

For the heat exchanger network design of S1, three possible layouts were simulated, as can be seen in Figure 8. A first possibility is the direct injection of the water in the compressor outlet (A), the second possibility is the injection of preheated water in the compressor outlet (B) and the final test case was the use of a saturation tower (the mHAT approach (C)). Next to these three proposed layouts (Figure 8), several additional layout, using additional heat exchangers (for instance an aftercooler and a second economizer to preheat the feedwater, as proposed by [16] in the mHAT plus cycle)

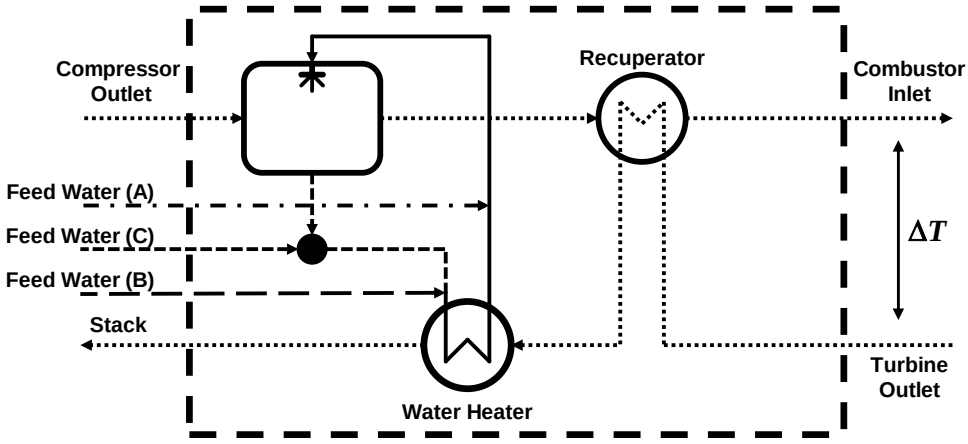

Figure 8: Heat exchanger network designs, using direct water injection (Case A), preheated water injection (Case B) and the use of a saturation tower (Case C).

are possible. These layout were however excluded from this study, since the maximum amount of heat exchangers was set to two in order to keep the cycle layout simple.

The simulations of case (B) are divided into two subcases. In a first subcase, water was heated, but the final injection temperature remained below the boiling point. In the second subcase, liquid water was heated, boiled and the raised steam was superheated (5 °C). For this subcase, where temperature at the boiling point remains constant, a different approach needed to be applied; the water heater has been split up in three parts: a water heater, a boiler and a super heater. Finally, injection of a liquid-vapour mixture was not considered.

Even though exergy analysis of the black box showed that injection up to 0.09 kg/s of water (surge limit of the compressor) still results in a global exergy efficiency and destruction below limits that can be found in literature [31], this potential cannot fully be explored with the three considered networks in this paper (Figure 8). The optimal network, corresponding to the limit found in the black box simulations, requires more heat exchangers, which will make the cycle too complex for mGT applications. The black box

Table 3: Results of heat exchanger network design, using different injection types.

	Case A	**Case B**		**Case C**
		liquid	**steam**	
T_{stack}	76 °C	62 °C	132 °C	82 °C
T_{mix}	63 °C	65 °C	172 °C	74 °C
$\dot{m}_{\text{water}}$	40 g/s	43 g/s	29 g/s	40 g/s
η_{el}	40.5 %	40.8 %	39.5 %	40.0 %
$\dot{Q}_{\text{CONDENS}}$	129 kW_{th}	127 kW_{th}	136 kW_{th}	134 kW_{th}
T_{CONDENS}	25.7 °C	25.7 °C	25.0 °C	25.4 °C

maximal water injection of 0.09 kg/s of water is never reached, because the simulated stack temperature of 53 °C can never be reached (Table 3) in one of the three considered networks. The limitation for the stack temperature is the temperature of the working fluid mixture after water injection in Case A and C, and the low amount of water that can be heated in Case B. For direct injection (Case A), the mixing temperature of the compressed air and the liquid water is still quit high (around 63 °C). The stack temperature cannot be lowered further than this mixing temperature, otherwise the composite curves will cross, which is prohibited. The same explanation as for Case A can be given for Case C, the mHAT. The temperature of the excess water leaving the saturation tower, which is rerouted to the water heater, will determine the lowest possible stack temperature. Hot flue gasses cannot be cooled below this temperature, which corresponds to the saturation temperature of the compressed air.

The reason why the simulated black box potential cannot be reached with the simple heat exchanger networks considered in this paper (Figure 8), is illustrated by the hot composite curve of the black box (Figure 9). When injecting 0.09 kg/s of water in the mGT cycle, water starts to condensate from the exhaust gasses once the temperature gets below 67.3°C. From this point, the temperature changes little, even though a large amount of heat is available due to the condensing water. To use this heat without violating the second law – without crossing composite curves – a lot of heat needs to be absorbed in the cold stream at low temperature. Since the 0.09 kg/s of feedwater at 15°C is the only available incoming stream of the network at low temperature, this cannot be accomplished with simple heat exchanger

networks. To be able to recover this energy, more complex networks, using multiple phase flow heat exchangers are necessary. These networks are however too complex and too expensive and thus not in line with the mGT usage objective.

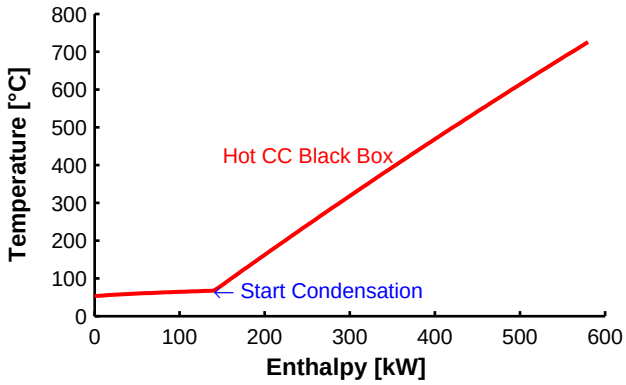

Figure 9: The very flat hot composite curve at low temperature, due to water condensation, makes that simple heat exchanger networks are not capable of reaching the black box potential, since not enough heat can be recovered at low temperature.

Final composite curves are shown in Figure 10. For all composite curves, only the heat exchange inside the actual heat exchangers is considered. The mixing is not taken into account, since mixing does not require a minimal pinch. For both the direct injection (Case A, Figure 10 (a)) and the mHAT case (Case C, Figure 10 (b)), the minimal pinch (10 °C) can be seen at the lowest temperature of the composite curves, meaning the difference between the stack and mixing temperature, which proves that the stack temperature is determined by the mixing temperature . For the indirect injection of steam (Case B steam), the minimal pinch depends on the boiling point of the water (Figure 10 (d)). If the stack temperature would be lowered, hot and cold composite curve would cross, which is prohibited. For the indirect injection of heated water (Case B water), the minimal stack temperature depends on the amount of water injected, since one should avoid the production of steam (Figure 10 (c)).

The lower the stack temperature becomes, the more water that can be injected, resulting in a higher electric efficiency (Table 3). Additionally, results of condensation simulations show that the lower the injected amount

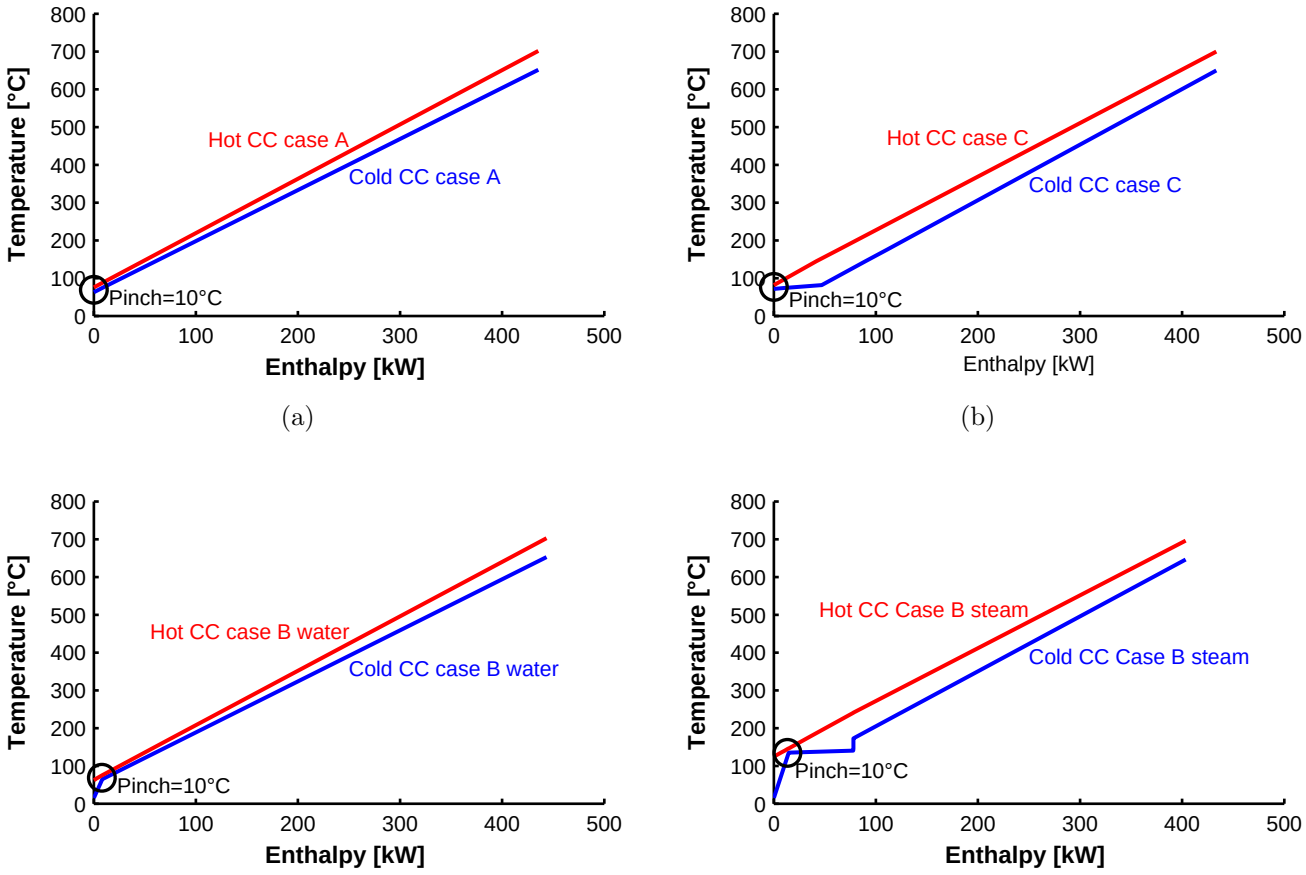

Figure 10: Composite curves of direct water injection (Case A) and the mHAT case (Case C) and the injection of heated water (Case B Water) and auto-raised steam (Case B Steam).

of water, the more the stack temperature needs to be lowered and the more heat needs to be disposed to the environment in order to make the cycle self-sufficient with water.

Injection of heated water is the most efficient way of water injection for waste heat recovery; however, differences between the different cases are rather small (Table 3). As mentioned before, electric efficiency is very sensitive to changing pressure losses. Increasing the pressure drop on the hot side

by 1 % will lower the electric efficiency by 0.37 % for case A, 0.37 % (liquid hot water injection) and 0.44 % (steam injection) for case B and 0.31 % for case C. These changes are the same order of magnitude as the difference in efficiency (Table 3). Therefore the results from Table 3 are only valid when heat exchangers with a cold and hot side pressure drop of 3 % and 40 mbar are implemented in the cycle. This maximal pressure drop will determine the final size of the heat exchanger, along with the necessary heat transfer surface. Regenerator investment cost is approximately 30 % of the total installation cost [39]. Traverso and Massardo showed that specific capital costs ranged from 125 $/kW to 190 $/kW [40]. This indicates that a different regenerator design will have a significant influence on the final total investment cost. Due to the small difference in efficiency, it might be possible that from an economic point of view, heated water injection is not the most optimal route for waste heat recovery in a mGT cycle. The design of the heat exchangers and full cost calculation is however outside the scope of this paper.

When the maximal amount of water is injected, by means of injection of heated water, the surge margin is reduced from 25 % to 16 %, which is still within the limits for power generation [33]. Similar surge behaviour was observed by Ferrari et al. and De Paepe et al. during steam injection experiments in the T100 mGT [18, 20]. This is due to a good design surge margin performance. The water fraction is limited to 6.7 wt%, which should still allow for a stable combustion [36]. Final stack temperature is 62 °C (Table 3), which is still above the dew point temperature of 52 °C (Figure 3). Although no possible problems are expected from the acidic environment created by the water condensation in the water heater or stack, some precautions such as the measures discussed in subsection 4.1 should be taken.

5. Conclusion

The results of a series of simulations of water injection in the compressor outlet of a mGT are presented. Water injection in the compressor outlet is a possible route for waste heat recovery in the mGT. The additional water will enhance the performance of the mGT, especially the electric efficiency. This will make the mGT as CHP more attractive for applications with a non-continuous heat demand. A two-step method was used, to find the thermodynamic optimal of the water injection. In the first step, the heat exchanger network of the mGT has been replaced by a black box system. Two

different scenarios were studied during this first step. In the first scenario, we investigated the maximal potential for water injection, by lowering the stack temperature, without violation of the second law of thermodynamics. In the second scenario, the cycle was made self-sufficient with water by condensing the water in the exhaust gasses; since the cost of the water consumption and treatment is a major drawback of humidified gas turbines. The final heat exchanger network was designed during step two of the two-step procedure by using composite curve theory.

Simulation performed on a Turbec T100 mGT, representative for mGTs, resulted in following results:

- Black box simulations indicated that 9 % absolute efficiency increase can be achieved by injecting 17 %wt of water (90 g/s) in the compressor exhaust without global violation of the second law of thermodynamics. By doing so, the remaining waste heat in the flue gasses is recovered, resulting in a final stack temperature of 53 °C.

- Composite curve theory and pinch analysis however showed that this theoretic potential cannot be achieved with a limited amount of heat exchangers (two). Lowering stack temperature until 53 °C is not possible, which limits the recovery of waste heat.

- The lowest possible stack temperature, depending on the injection type is 76 °C (direct injection of water), 62 °C (direct injection of heated water) and 82 °C (mHAT). These stack temperature respectively corresponded to an injection of 40 g/s, 43 g/s and 40 g/s of water, which resulted in absolute efficiency increases of 4.3 %, 4.6 % and 3.8 %.

- To make the cycle fully self-sufficient for water, the flue gasses need to be cooled to lower the stack temperature below 26°C. Below this temperature, enough water will condensate from the flue gasses to compensate for the injected water.

From a thermodynamic point of view, direct injection of heated water is identified as the most optimal cycle layout for waste heat recovery through water injection in a mGT. The most waste heat can be recovery in this injection scheme, resulting in the lowest stack temperature. The difference in efficiency increase between the different injection schemes is however rather limited. Taking into account economic parameters, like investment costs and electricity and natural gas prices, might lead to a different optimal design.

6. Acknowledgement

The research was funded by the Research Foundation Flanders - FWO.

Nomenclature

Abbreviations

BB Black Box

CHP Combined Heat and Power

GT Gas Turbine

HAT Humid Air Turbine

ICE Internal Combustion Engine

mGT micro Gas Turbine

mHAT micro Humid Air Turbine

PIT Turbine Inlet Pressure, Pa

REVAP® REgenerative EVAPoration

S1 Scenario 1

S2 Scenario 2

TIT Turbine Inlet Temperature, °C

TOT Turbine Outlet Temperature, °C

WAC Water Atomizing inlet Cooling

Symbols

$\dot{E}x$ exergy flow, kW

β pressure ratio

$\dot{m}$ mass flow rate, kg/s

$\dot{Q}$ heat flux, kW

η efficiency, %

A turbine inlet cross section, m^2

k heat capacity ratio, (c_p/c_v)

R gas constant, 8.314 J/molK

T temperature, °C

Subscripts

CONDENS condensor

COOLER cooler

el electric

fuel fuel (in this case methane)

gain flow gaining exergy

HEATER heater

in ingoing flow

is isentropic

loss flow loosing exergy

mix condition of mixing point

out outgoing flow

stack condition of stack flow

turb condition inside turbine

water condition of water flow

superscripts

dest destruction

eff efficiency

References

[1] U.S. Department of Energy, Office of Energy Efficiency & Renewable Energy, Office of Power Technologies, Advanced Microturbine Systems – Program plan for fiscal years 2000 through 2006, Technical Report, U.S.A., 2000.

[2] P. A. Pilavachi, Mini- and micro-gas turbines for combined heat and power, Applied Thermal Engineering 22 (2002) 2003 – 2014.

[3] F. Delattin, S. Bram, S. Knoops, J. De Ruyck, Effects of steam injection on microturbine efficiency and performance, Energy 33 (2008) 241 – 247.

[4] C. F. McDonald, Recuperator considerations for future higher efficiency microturbines, Applied Thermal Engineering 23 (2003) 1463 – 1487.

[5] L. Goldstein, B. Hedman, D. Knowles, S. I. Freedman, R. Woods, T. Schweizer, Gas-Fired Distributed Energy Resource Technology Characterizations, National Renewable Energy Laboratory, Oak ridge, Tennessee, U.S.A., 2003.

[6] C. F. McDonald, C. Rodgers, Ceramic recuperator and turbine: The key to achieving a 40 percent efficient microturbine, ASME Conference Proceedings 2005 (2005) 963–971.

[7] S. Campanari, E. Macchi, Technical and tariff scenarios effect on microturbine trigenerative applications, Journal of Engineering for Gas Turbines and Power 126 (2004) 581–589.

[8] M. T. Kim, S. W. Lee, Application of in situ oxidation-resistant coating technology to a home-made 100kw class gas turbine and its performance analysis, Applied Thermal Engineering 40 (2012) 304 – 310.

[9] G. Lagerström, M. Xie, High performance and cost effective recuperator for micro-gas turbines, in: ASME Conference Proceedings, ASME paper GT2002-30402, 2002, pp. 1003–1007.

[10] C. F. McDonald, Low-cost compact primary surface recuperator concept for microturbines, Applied Thermal Engineering 20 (2000) 471 – 497.

[11] L. Galanti, A. F. Massardo, Micro gas turbine thermodynamic and economic analysis up to 500kWe size, Applied Energy 88 (2011) 4795 – 4802.

[12] M. Jonsson, J. Yan, Humidified gas turbines – a review of proposed and implemented cycles, Energy 30 (2005) 1013 – 1078.

[13] J. J. Lee, M. S. Jeon, T. S. Kim, The influence of water and steam injection on the performance of a recuperated cycle microturbine for combined heat and power application, Applied Energy 87 (2010) 1307 – 1316.

[14] S. Dodo, S. Nakano, T. Inoue, M. Ichinose, M. Yagi, K. Tsubouchi, K. Yamaguchi, Y. Hayasaka, Development of an advanced microturbine system using humid air turbine cycle, in: ASME conference proceedings, ASME paper GT2004-54337, 2004, pp. 167–174.

[15] K. Mochizuki, S. Shibata, U. Inoue, T. Tsuchiya, H. Sotouchi, M. Okamoto, New concept of a micro gas turbine based co-generation package for performance improvement in practical use, in: ASME conference proceedings, ASME Paper PWR2005-50364, 2005, pp. 1305–1310.

[16] J. Parente, A. Traverso, A. F. Massardo, Micro humid air cycle: Part A – thermodynamic and technical aspects, in: ASME conference proceedings, ASME paper GT2003-38326, 2003, pp. 221–229.

[17] J. Parente, A. Traverso, A. F. Massardo, Micro humid air cycle: Part B – thermoeconomic analysis, in: ASME conference proceedings, ASME paper GT2003-38328, 2003, pp. 231–239.

[18] M. L. Ferrari, M. Pascenti, A. N. Traverso, A. F. Massardo, Hybrid system test rig: Chemical composition emulation with steam injection, Applied Energy 97 (2012) 809 – 815. ¡ce:title¿Energy Solutions for a Sustainable World - Proceedings of the Third International Conference on Applied Energy, May 16-18, 2011 - Perugia, Italy¡/ce:title¿.

[19] C. Wei, S. Zang, Experimental investigation on the off-design performance of a small-sized humid air turbine cycle, Applied Thermal Engineering 51 (2013) 166 – 176.

[20] W. De Paepe, F. Delattin, S. Bram, J. De Ruyck, Steam injection experiments in a microturbine – a thermodynamic performance analysis, Applied Energy 97 (2012) 569 – 576.

[21] W. De Paepe, F. Delattin, S. Bram, J. De Ruyck, Water injection in a micro gas turbine – Assessment of the performance using a black box method, Applied Energy 112 (2013) 1291–1302.

[22] S. Bram, J. De Ruyck, Exergy analysis tools for aspen applied to evaporative cycle design, Energy Conversion and Management 38 (1997) 1613 – 1624.

[23] A. D. Rao, Process for producing power. US patent no. 4829763, 1989.

[24] S. Bram, J. De Ruyck, Humid air cycle development based on exergy analysis and composite curve theory, ASME Conference Proceedings 1995 (1995) 95–CTP–39.

[25] Turbec AB, T100 microturbine CHP system: Technical description ver 4.0, 2000-2001.

[26] W. De Paepe, F. Delattin, S. Bram, F. Contino, J. De Ruyck, A study on the performance of steam injection in a typical micro Gas Turine, in: ASME conference proceedings, ASME paper GT2013-94569, 2013, p. 10 pages.

[27] Aspen Technology Inc., Aspen plus version 2006.5, 2006. URL: `www.aspentech.com`, accessed: 2014-01-23.

[28] Y. Çengel, M. Boles, Thermodynamics: an engineering approach, McGraw-Hill series in mechanical engineering, McGraw-Hill Higher Education, Boston, US, 2006.

[29] U. Desideri, F. Di Maria, Water recovery from hat cycle exhaust gas: a possible solution for reducing stack temperature problems, International Journal of Energy Research 21 (1997) 809–822.

[30] M. De Paepe, E. Dick, Technological and economical analysis of water recovery in steam injected gas turbines, Applied Thermal Engineering 21 (2001) 135 – 156.

[31] M. A. El-Masri, A modified, high-efficiency, recuperated gas turbine cycle, Journal of Engineering for Gas Turbines and Power 110 (1988) 233–242.

[32] M. Ebrahim, Al-Kawari, Pinch technology: an efficient tool for chemical-plant energy and capital-cost saving, Applied Energy 65 (2000) 45 – 49.

[33] P. Walsh, P.P. Fletcher, Gas turbine performance, Blackwell Science Publications, Oxford, UK, 2004.

[34] W. Day, B. kendrick, D knight, A. Bhargava, W. Sowa, M. Colket, K. Casleton, D. Maloney, Hat cycle technology development program, in: Advanced turbine systems annual program review meeting, 1999, pp. 2–8. URL: `www.netl.doe.gov/publications/proceedings/99/99ats/2-8.pdf`, accessed: 2014-01-23.

[35] A. A. Belokon, K. M. Khritov, L. A. Klyachko, S. A. Tschepin, V. M. Zakharov, J. George Opdyke, Prediction of combustion efficiency and NO_x levels for diffusion flame combustors in hat cycles, ASME Conference Proceedings 2002 (2002) 791–797.

[36] F. Hermann, J. Klingmann, R. Gabrielsson, Computational and experimental investigation of emissions in a highly humidified premixed flame, ASME Conference Proceedings 2003 (2003) 819–827.

[37] E. Macchi, A. Poggio, Cogeneration plant based on a steam injection gas turbine with recovery of the water injected: design criteria and initial operating experience, in: ASME-IGTI TURBO conference Proceedings, ASME paper 94-GT-17, 1994, pp. 1–10.

[38] N. D. Ågren, M. O. Westermark, M. A. Bartlett, T. Lindquist, First experiments on an evaporative gas turbine pilot power plant: Water circuit chemistry and humidification evaluation, Journal of Engineering for Gas Turbines and Power 124 (2002) 96–102.

[39] Rodgers, 25-5 kWe microturbine design aspects, in: ASME Conference proceedings, ASME paper number 200-GT-626, 2000, pp. 1–11.

[40] A. Traverso, A. F. Massardo, Optimal design of compact recuperators for microturbine application, Applied Thermal Engineering 25 (2005) 2054 – 2071.